Change of exposure time mid-test in high temperature DIC measurement

OPEN ACCESS
IOP Publishing
Measurement Science and Technology
Meas. Sci. Technol. **31** (2020) 075402 (11pp)
https://doi.org/10.1088/1361-6501/ab7bbf

Change of exposure time mid-test in high temperature DIC measurement

Thinh Q Thai[1], Adam J Smith[1], Robert J Rowley[1], Paul R Gradl[2] and Ryan B Berke[1]

[1] Mechanical and Aerospace Engineering, Utah State University, 4130 Old Main Hill, Logan, UT 84322-4130, United States of America
[2] NASA, Marshall Space Flight Center, Huntsville, AL 35812, United States of America

E-mail: ryan.berke@usu.edu

Received 24 November 2019, revised 11 February 2020
Accepted for publication 2 March 2020
Published 27 April 2020

Abstract

Performing digital image correlation (DIC) at extreme temperatures has been greatly challenging due to the radiation which saturates the camera sensor. At such high temperatures, the light intensity emitted from an object is occasionally so powerful that the acquired images are overwhelmingly saturated. This induces data loss, potentially ruining the test, thus requiring the user to restart the test. For this reason, selection of an appropriate camera sensitivity plays a crucial role prior to beginning the test. Exposure time is a factor contributing to camera sensitivity and it is the easiest setting to manipulate during the test since it introduces minimal errors when comparing to other factors, especially in quasi-static tests. This paper examines the influence of changing exposure time mid-test on DIC measurement uncertainty. The investigation was conducted by rigid body motion experiments at room temperature and 1600 °C, respectively. Thereby, some recommendations are given to help DIC users assess their images at room temperature to extrapolate the exposure at extreme temperatures along with accompanying solutions to salvage data at high temperature.

Keywords: DIC, extreme temperature, exposure time, ultraviolet light, graphite, Gleeble

(Some figures may appear in colour only in the online journal)

1. Introduction

Acquisition of deformation and strain measurements is an important step in designing engineering applications, but deformation and strain are frequently non-uniform. In such cases, it is necessary to get a full field strain map for the purpose of material characterization. Digital image correlation (DIC) [1, 2] is a non-contacting method which is widely used to obtain full field strain maps by comparing images acquired from high resolution cameras before and after deformation. DIC has many advantages [3, 4], including (i) it is non-contact, (ii) it is able to collect full field data and (iii) it can be applied in a broad range of length scales from nanoscale [5, 6] to meter-scale [7, 8] as long as appropriate camera and lenses are provided.

To make meaningful image comparisons, it is pivotal to acquire images with sufficient monochromatic grayscale contrast [9]. There are four main methods to control image contrast [10] including (i) the aperture on the lens, (ii) the exposure time of the camera, (iii) the intensity of the supplied light source and (iv) the gain of the camera amplifier. Each method has its own pros and cons and, depending on testing conditions, one method could be technically superior to others. For example, during a dynamic test, exposure time must be kept short to avoid motion blur, but during a quasi-static test, exposure time is allowed to be variable [11].

When performing DIC at temperatures above 550 °C, one of the primary challenges is the glowing of objects from black body radiation which deteriorates image contrast [12, 13]. It is known that the radiation is much brighter at longer wavelengths (i.e. red and infrared) than it is at shorter wavelengths (i.e. blue and ultraviolet (UV)). Researchers

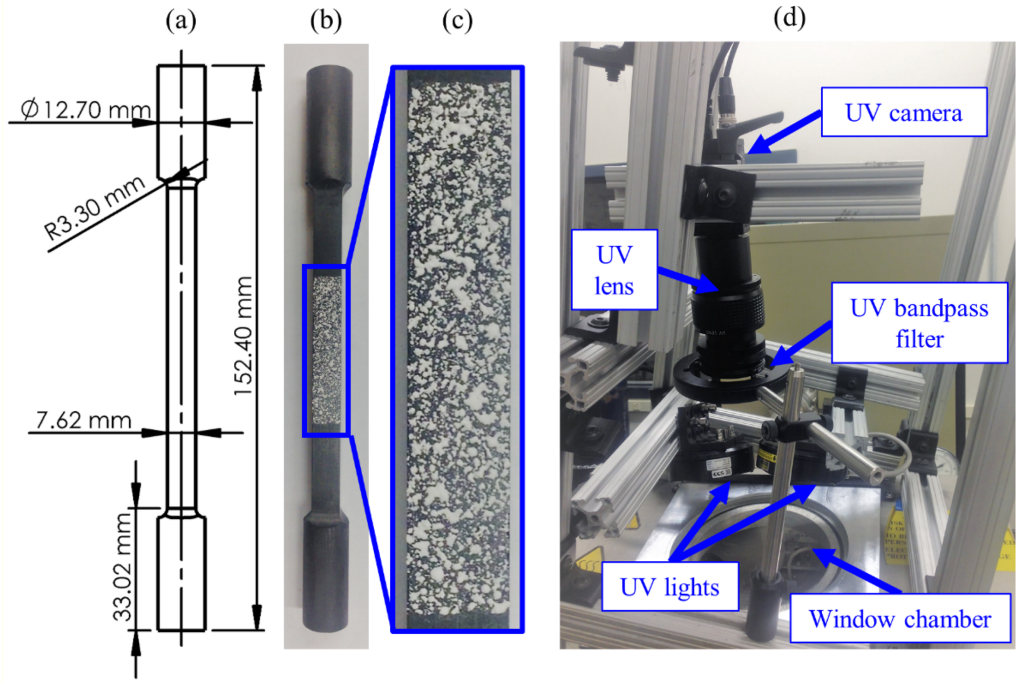

Figure 1. (a) A specimen schematic, (b) a photograph of testing specimen, (c) a magnification of speckle pattern and (d) experimental setup of UV optics imaging system.

[14–16] have used a blue band-pass filter and external blue illumination to screen out some of the brightest glow, raising the temperature limit at which DIC can be applied without oversaturation to as high as 2000 °C [17]. Berke and Lambros introduced a novel variation of DIC named UV-DIC [18], which utilizes UV optics in order to increase the temperature limit even further compared to blue. Under the camera settings used in that study, blue-filtered DIC saturated at as low as 900 °C while UV-DIC remained minimally saturated to at least 1125 °C. UV-DIC has since been demonstrated to at least 1600 °C [19] but its upper temperature limit remains unknown. Thanks to its shorter wavelength, UV-DIC can potentially perform to even higher temperatures than the 2000 °C reported for blue-filtered DIC.

Recently, Thai *et al* [19] recognized that the upper temperature limit of DIC depends on the camera's sensitivity to light. In that paper, he proposed a normalized metric called Delta (Δ) as a general guideline for setting the exposure time of cameras with different sensitivity. However, his recommendation only considered how to select exposure time at the beginning of a test, which is then left constant for the duration of the test. High temperature tests are expensive and unpredictable, and in some cases, the specimen may emit more light than anticipated prior to testing. The image contrast is thus degraded by powerful radiation, so maintaining the initial exposure time during the whole test becomes unfeasible. By changing the exposure time during mid-test, DIC users may still be able to get some meaningful data instead of being presented with no data or restarting the experiment.

In this paper, we investigate the influence on DIC measurement uncertainty when changing exposure time during a test. Compared to paper [19], in which camera settings (e.g. exposure time) were selected prior to performing high temperature tests and remained constant, this paper emphasizes changing exposure time *in situ* during the course of measurement. The effect on DIC measurement is then examined (i) when both images are taken at room temperature; (ii) when both images are taken at high temperature; and (iii) when the reference image is at room temperature but the deformed image is at high temperature. Experiments were performed at room temperature (RT) and 1600 °C, respectively. Having done so, some suggestions are given to DIC users about the alteration of exposure time during a test.

2. Methods

Specimens as shown schematically in figure 1(a) were machined from super fine grain, high density, extruded graphite rods purchased from Graphtek LLC. The rods had a length of 152.4 mm (6 in) and diameter of 12.7 mm (0.5 in). A square cross section of 7.62 mm (0.3 in) was machined in order to provide a flat, planar surface on which to perform DIC. The graphite was chosen as the material since it is inexpensive, easily machinable, and has a melting point of 3000 °C in vacuum which is beyond the highest temperature in this work (1600 °C). A white speckle pattern as shown in figures 1(b) and (c) was applied using Pyro-Paint 634-AL from Aremco Products Inc. which has a maximum temperature rating of 1760 °C, also above the highest temperature explored in this work. The white speckle pattern was applied directly on the graphite's naturally dark background by a splattering method. Prior to testing, the paint was dried at room temperature for 2 h and then cured at 93 °C (200 °F) for 2 h according to the manufacturer's manual. Additionally, an optical imaging

system including a UV camera, UV lens, UV lights and UV filter was mounted on a T-slot fixture as shown in figure 1(d). More information on the camera system and related optics can be found in [19].

Due to the aggressive oxidation of graphite in air environments, all high-temperature testing was performed in vacuum using a Gleeble 1500D thermo-mechanical system, which heats electrically-conducting specimens via joule heating. A K-type thermocouple was used as feedback control during temperature heating. However, K-type thermocouples are only rated to 1250 °C [20] while tests were performed up to 1600 °C. For this reason, a modified method was introduced to heat beyond the range of the K-type thermocouple. Since the two ends of specimen were held by cooled grips, a thermal gradient results along the axis of the specimen, with the hottest temperature occurring in the middle of specimen. The specimen was heated twice: first with two thermocouples, TC1 in the middle and TC2 at one end, until TC1 reached a maximum temperature of 1250 °C. This established a linearly proportional relationship between the temperatures recorded by the two thermocouples. TC1 was then removed so to not block any cameras' view of the surface for DIC, and TC2 was used for feedback control. More details were presented in [19]. Figure 2 shows a thermal image of a heated specimen captured from a FLIR A6751sc IR camera. As can be seen from the figure, the temperature is highest in the middle at 1600 °C and decreases steadily towards two ends. Temperatures are linearly proportional to those observed at lower temperatures by both thermocouples.

In order to investigate the effect of only exposure time, all other parameters contributing to camera sensitivity (i.e. UV light intensity, aperture, and gain) remained unchanged. Specifically, the UV light intensity was set to around 60%, the aperture of the lens was 4 and the gain of the camera was 0. The specimen was tested at two different temperature levels: room temperature (RT) and 1600°C. No loads were applied throughout testing. At each temperature level (RT and 1600 °C) and at each of value of exposure time (totaling 12 values spanning the full capability of the camera from 500 μs to 61 000 μs), two consecutive images at the same state were taken. In total, $12 \times 2 = 24$ images were captured at room temperature and 24 more at high temperature corresponding to Experiment A and Experiment B in the Results Section.

Images were then processed using VIC-2D (version 2009), a commercial DIC algorithm from Correlated Solutions Inc. As summarized in table 1, an image at each of the 12 exposure times was correlated against a second image at each of the 12 exposure times, such that each use of VIC-2D involved only 2 images and the analysis was performed $12 \times 12 = 144$ times for a given temperature. Three cases were studied: (A) both images at room temperature (144 image pairs), (B) both images at 1600 °C (144 more image pairs), and (C) a reference image at room temperature correlated with a deformed image at 1600 °C (144 more image pairs). In every correlation, the subset size was 61×61 pixels, the step size was 25 pixels, and the strain window was 15 subsets. The majority of the image pairs did not correlate, and are excluded from the presented data.

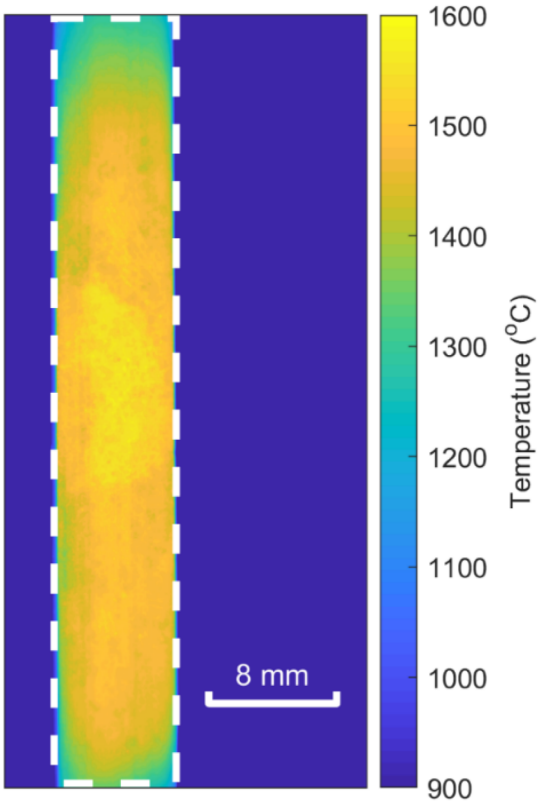

Figure 2. The thermal map at 1600 °C taken by FLIR IR camera, vertical color bar displays temperature (°C) scale inside white dashed rectangle.

Table 1. Summary of image pairs used in correlations.

	Reference image		Deformed images		Image pairs
A	12 exposure times at RT	×	12 exposure times at RT	=	144 image pairs
B	12 exposure times at 1600 °C	×	12 exposure times at 1600 °C	=	144 image pairs
C	12 exposure times at RT	×	12 exposure times at 1600 °C	=	144 image pairs

Next, the output from VIC-2D was post-processed by MATLAB to compute the mean strain and 95% confidence interval. Since no load was applied, all strain should be nominally zero at any fixed temperature. The mean strain is an indicator of the accuracy of DIC under changing exposure times, while the confidence interval is an indicator of precision. The 95% confidence interval was computed by sorting the strain data in ascending order, then calculating the distance between the 2.5% and 97.5% thresholds of the data.

Exposure time varies from camera to camera. For example, high speed cameras have short exposure time while the slower-speed UV cameras used in this study lean towards longer exposure time. For this reason, a metric of image contrast, Δ, was introduced in order to let DIC users know how to choose

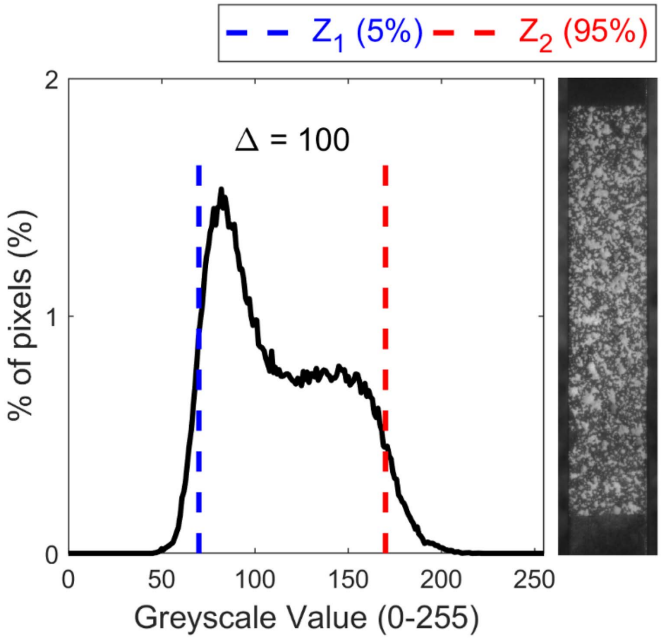

Figure 3. Example of 90% confidence interval approach with respective speckle pattern, using room temperature data at exposure time of 20 000 µs.

an appropriate exposure time value which can be applied to any camera. A detailed computing procedure was presented in [19], but is summarized as follows. The contrast $\Delta = Z_2 – Z_1$ is the difference in grey values between a 'typical' dark speckle (Z_1) and a 'typical' bright speckle (Z_2), as recommended by Phillip Reu [21]. In this case, Z_1 and Z_2 are selected by the range of the median 90% of pixels in the image. As illustrated in figure 3, the histogram is integrated from 0 until reaching 5% of the total pixels, and that greyscale value represents a 'typical dark pixel' which is called Z_1. Similarly, the histogram is integrated from 0 until reaching 95% of the total pixels, and that greyscale value represents a 'typical bright pixel' called Z_2. A 'good' contrast is when $\Delta \geq 50$ [22] and $Z_2 < 255$ (less than 5% of saturated pixels) for an 8-bit camera.

Table 2 shows the Z_1, Z_2, and Δ for each of the 12 exposure times at RT and 1600 °C, respectively. In general, Z_1 and Z_2 increase with higher temperature and higher exposure times until Z_2 reaches 255 (saturation). Consequently, Δ decreases at very high exposure times. The table also shows the percentage of pixels which are saturated in each of the images. Note that whenever this percentage is 5 or larger, Z_2 is always 255.

3. Results

3.1. Change of exposure time during isothermal testing (room temperature)

Figure 4 shows all pairs in which images at room temperature are able to be correlated against each other. There are 27 pairs which are successfully corelated in the total of 144 pairs as introduced in table 1 at room temperature. The blue dashed

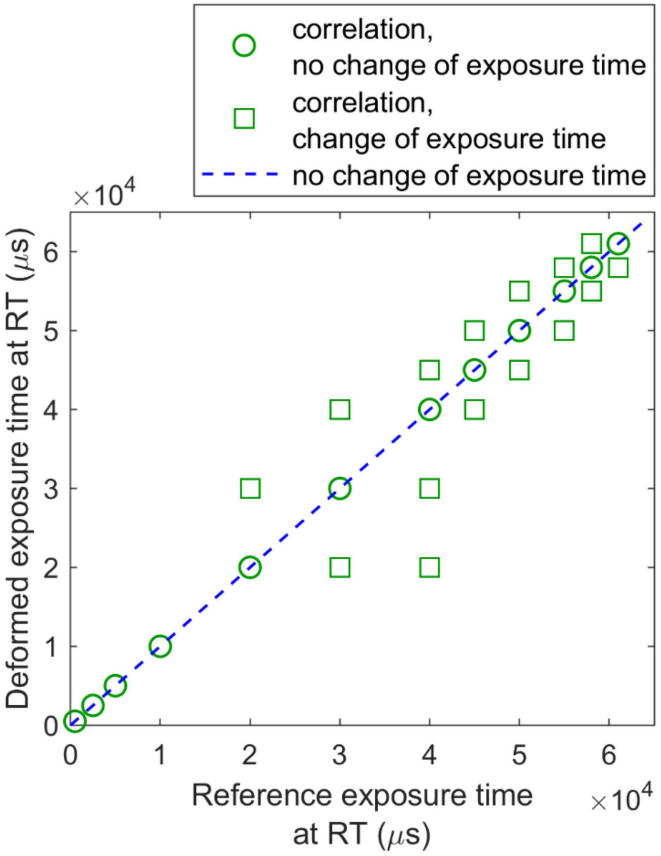

Figure 4. Image pairs which successfully correlated at room temperature.

line indicates no change of exposure time. It can be seen that for low exposure times (10 000 µs and below in this paper), exposure time cannot be changed. However, for high reference exposure times, exposure time can be changed and higher reference exposure times give narrower ranges of alteration.

Figure 5 shows the (a) axial displacement u and (b) axial normal strain ε_{xx} measured by DIC for each correlation pair from figure 4, along with the 95% uncertainty band. Only the image pairs which successfully correlated are included in the figure. The legend indicates the reference exposure time while the horizontal axis indicates the exposure time of the deformed images. For any data points having the same value of exposure time, they are displaced slightly in order to avoid excessive overlapping of data markers. The experiment was purely static, therefore u displacement and strain ε_{xx} should both nominally be zero. As can be confirmed from figure 5, zero falls within the 95% uncertainty bands of about 95% of all displacement and strain measurements, which is in good agreement with no applied loading. Due to the similarity in results of u displacement and strain ε_{xx}, only strain ε_{xx} are presented in the subsequent figures to keep the writing to be more concise. Furthermore, as the mean strains are all nominally zero, subsequent figures will compare just the sizes of the uncertainty bands instead of showing full-range of the uncertainty bands.

In order to present results which can be generalized to other cameras, the exposure times of the deformed images

Table 2. Raw data of Δ calculation at RT and 1600 °C.

	Room temperature				1600 °C			
Exposure time	Z_1	Z_2	Δ	% of saturated pixels	Z_1	Z_2	Δ	% of saturated pixels
500 μs	8	12	4	0	9	12	3	0
2500 μs	15	28	13	0	19	31	12	0
5000 μs	23	49	26	0	30	55	25	0
10 000 μs	38	89	51	0	53	103	50	0
20 000 μs	70	170	100	0	99	196	97	0
30 000 μs	100	249	149	3.57	144	255	111	20.00
40 000 μs	131	255	124	31.41	190	255	65	56.10
45 000 μs	146	255	109	41.45	213	255	42	73.83
50 000 μs	161	255	94	49.86	236	255	19	88.28
55 000 μs	176	255	79	57.81	255	255	0	95.85
58 000 μs	185	255	70	62.81	255	255	0	97.92
61 000 μs	194	255	61	67.96	255	255	0	98.93

have been converted into Δ as shown in figure 6. The vertical axis is the size of the 95% uncertainty band while the horizontal axis is Δ of the deformed images. It can be inferred that of the image pairs studied, when $\Delta < 50$ the exposure time is unable to change and still successfully correlate between two images. If $\Delta > 50$, it is possible to change exposure time, but the size of the uncertainty band always increases to result in V-shaped plots. In cases when there is no change of exposure time, higher Δ generally gives lower uncertainty.

Figure 7 shows the relationship between the size of the uncertainty band vs how far Δ is changed. It can be deduced that at higher reference exposure times, a minor variation of Δ results in a marked increase in uncertainty. This is demonstrated in figure 7 thanks to the steeper slope of the dashed lines at longer reference exposure times.

Figure 8 is a further investigation where the slope of the data in figure 7 is compared to Δ of the reference images. Overall, once $Z_2 = 255$, longer reference exposure times lead to smaller Δ and higher slope.

3.2. Change of exposure time during isothermal testing (extreme temperature—1600 °C)

The testing in this section is similar to Result A with the only difference being that the tests were performed at 1600 °C. At such high temperatures, the specimen emits light in the form of blackbody radiation which can saturate the recorded images [18]. For this reason, there are 10 pairs which are successfully correlated in the total of 144 pairs as shown in figure 9. This is lower when compared to the 27 successfully correlated pairs at room temperature. For the camera equipment and settings used in this study, images with exposure times above 45 000 μs were too saturated to perform DIC, regardless of which other images they were correlated against as indicated by the red shaded region in figure 9. Accordingly, only exposure times of 45 000 μs and below are plotted in this section.

Figure 10 presents the 95% uncertainty band of (a) u displacement and (b) strain ε_{xx} during alteration of exposure time at 1600 °C, comparable to figure 5. The exposure time of the reference images are listed in the legend of the figure. In general, all displacements and strains are centered around zero which matches the condition of no applied loading. This is demonstrated that the 95% uncertainty bands cover zero in about 95% of all measurements which is in good agreement with the definition of 95% uncertainty band. Once again, only the size of the uncertainty bands in figure 10(b) are reported in subsequent figures.

Figure 11 shows the conversion of the exposure time from the deformed image to Δ at 1600°C, similar to the result of figure 6 at room temperature. Once again, if the initial $\Delta < 50$, there is no chance for two images of different exposure times to be correlated. At high temperature, there is less chance for two images of different exposure times to be correlated due to the considerable decrease of how many images have $\Delta > 50$. In this data set, only two image pairs with differing exposure times are able to correlate, so no further examination of slopes is performed.

3.3. Change of exposure time during mid test (i.e. different temperatures)

In this section, the analysis of the previous two sections is repeated again, using a reference image at room temperature and a deformed image at 1600 °C. Compared to the previous high temperature result (Result B), in which all exposure times over 45 000 μs failed to correlate, figure 12 shows that exposure times of 50 000 μs and 61 000 μs at room temperature were able to correlate against images at 30 000 μs and 40 000 μs, respectively. Similarly, initial exposure times of 30 000, 40 000, and 45 000 μs at room temperature were unable to correlate against images at the same exposure time at high temperature, but were able to correlate with other images at reduced exposure times. For the cameras used in this paper, all initial exposure times exceeding 20 000 μs at room temperature are required to reduce at high temperature in order to get successful correlation. Otherwise, they lose correlation due to saturation as indicated by the red shaded region in figure 12.

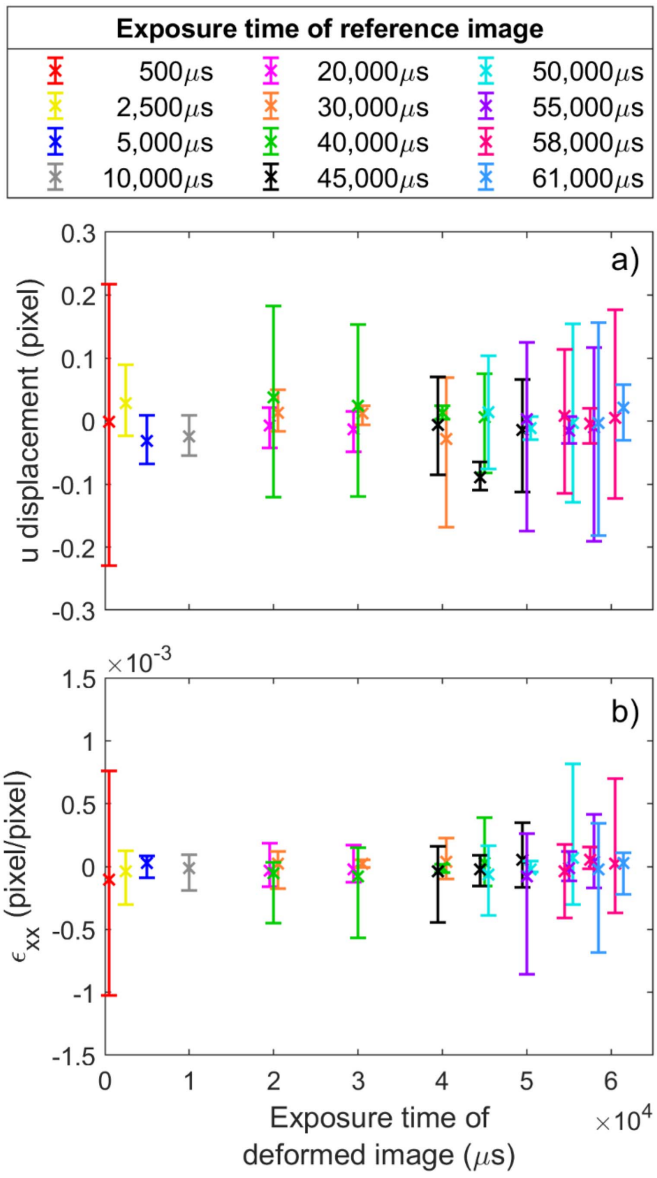

Figure 5. 95% uncertainty band when changing exposure time at room temperature illustrated by (a) u displacement and (b) strain ε_{xx}.

Figure 13 adopts the identical approach of figure 5 at room temperature as well as figure 10 at high temperature. However, the mean displacement and strain are no longer zero indicating non-uniform thermal expansion which takes place between the reference and deformed images. Consequently, the size of the uncertainty band is no longer a meaningful metric of measurement uncertainty, so no analysis of slopes is performed. Instead, figure 14 shows the non-uniform thermal strain due to the non-uniform temperature gradients as demonstrated in figure 2.

4. Discussion

In our previous paper [19], we recommended two criteria for good contrast when performing DIC at extreme temperature. First, at room temperature the exposure time should be kept as small as possible while maintaining $\Delta > 50$, leaving the most room for Z_1 and Z_2 to increase as the images brighten at high temperature. Second, we recommended avoiding any images in which Z_2 equals the maximum value of the sensor (255 for an 8-bit camera), as this would indicate that over 5% of all pixels have already saturated at the start of the test, and contrast can only worsen with increasing temperature. In that study, exposure time remained constant for each image pair.

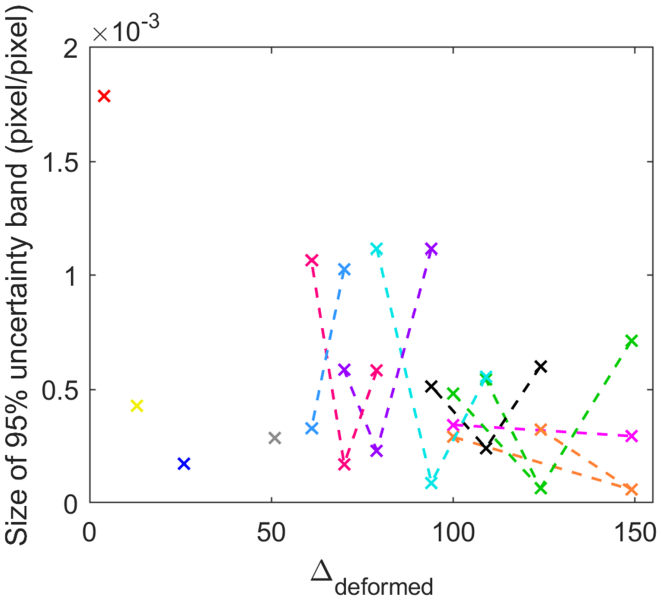

Figure 6. Influence of changing exposure time on uncertainty band at RT illustrated via Δ. The reference images are indicated using the same legend as in figure 5.

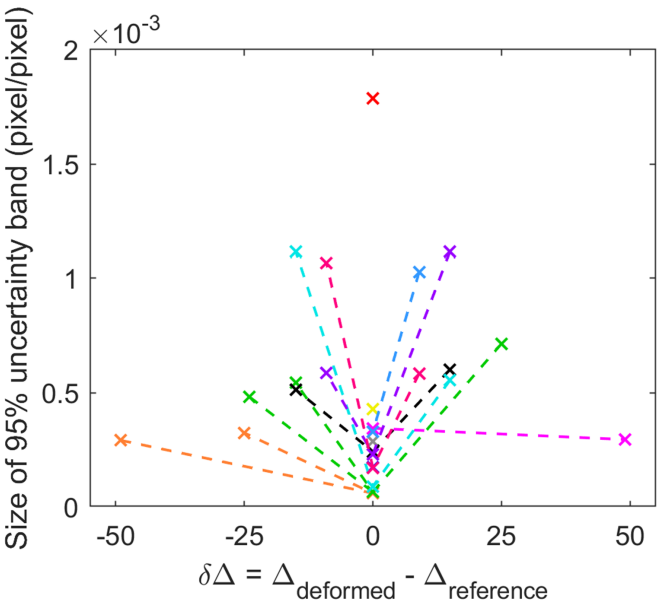

Figure 7. Relationship of 95% uncertainty band and Δ variation at various exposure times. The reference images are indicated using the same legend as in figure 5.

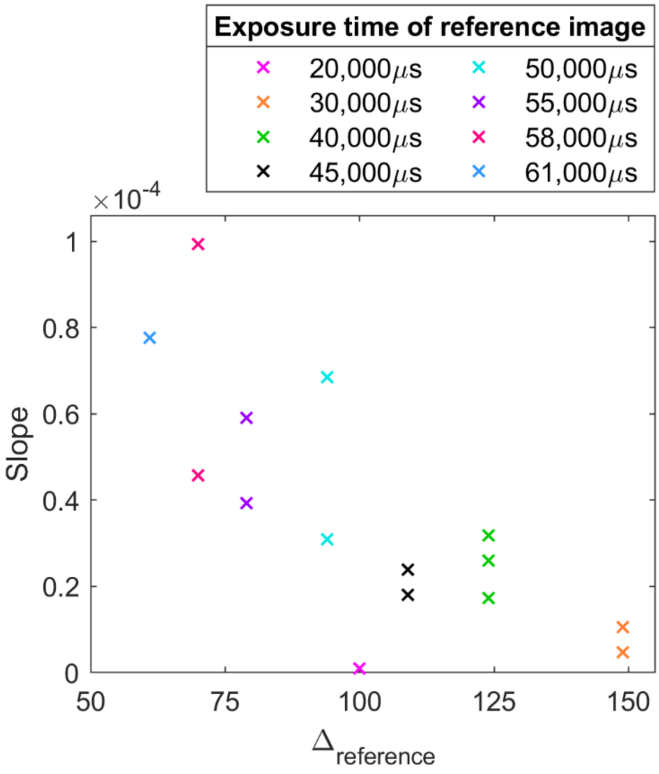

Figure 8. Investigation of slope with respect to Δ of reference images.

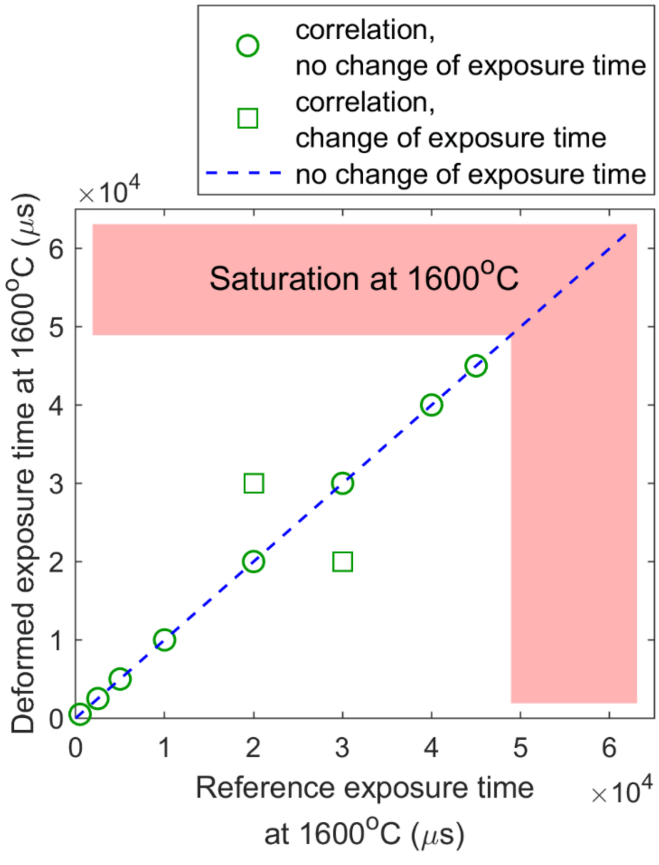

Figure 9. Image pairs which successfully correlated at 1600°C.

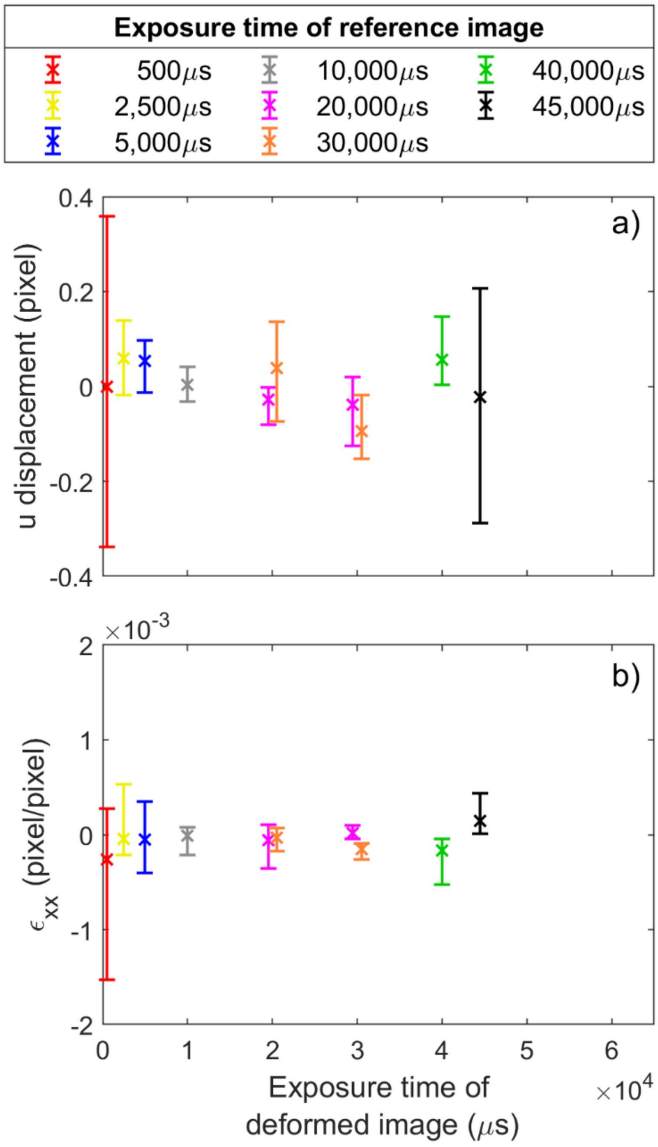

Figure 10. 95% uncertainty band when changing exposure time at 1600 °C illustrated by (a) *u* displacement and (b) strain ε_{xx}.

It can be inferred from figures 4 and 5 that there is no possibility of changing exposure time even at RT when initial exposure time is set too low ($\leqslant$ 10 000 μs for the camera in this paper). The reason comes from the excessive darkness of the images, as is demonstrated at low values of Δ in figure 6. This confirms that, of the image pairs studied, there is no chance to alter exposure time if $\Delta < 50$. When $\Delta > 50$, it becomes possible to change exposure time within a limited range from the reference exposure time, but the uncertainty band becomes larger as demonstrated by the V-shaped plots in figure 6. This is reasonable since varying the exposure time of the correlated images leads to a change of contrast which results in higher uncertainty of the DIC algorithm. In general, higher Δ gives a smaller uncertainty and allows for modest changes in exposure time.

Figures 7 and 8 further explore how far exposure time can be changed from the initial value at a fixed temperature. In

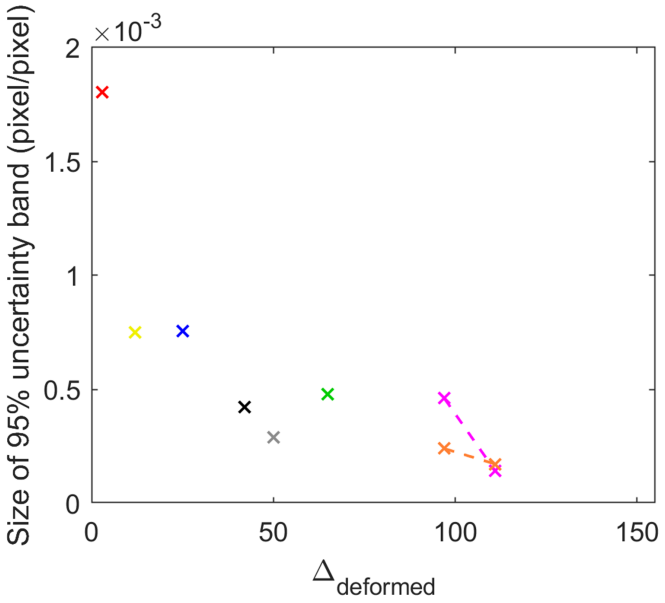

Figure 11. Influence of changing exposure time on uncertainty band at 1600 °C illustrated via Δ. The reference images are indicated using the same legend as in figure 10.

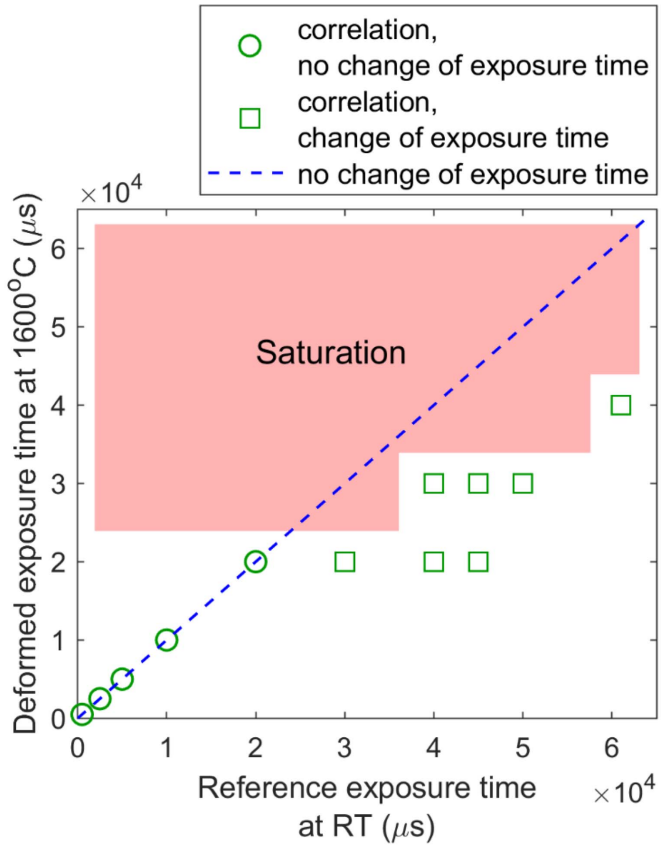

Figure 12. Image pairs which successfully correlated at RT vs 1600 °C.

general, larger initial values of Δ have more space to change exposure time and show a smaller increase of uncertainty when exposure time is changed. Additionally, when changing

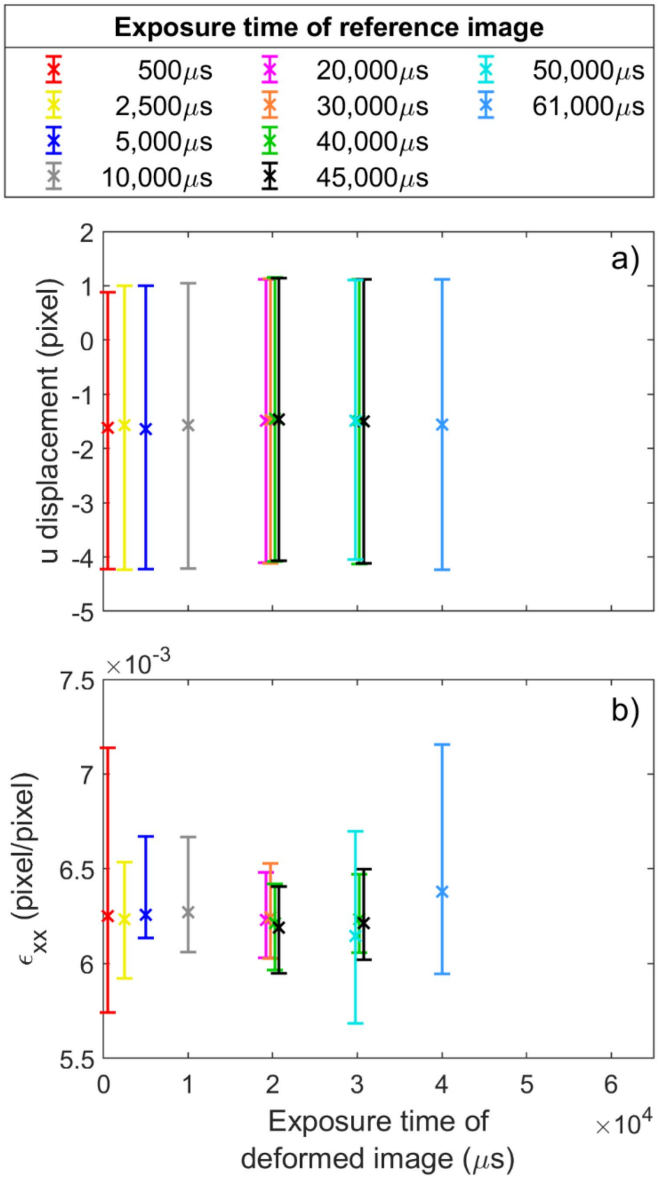

Figure 13. 95% uncertainty band when changing exposure time during mid test illustrated by (a) u displacement and (b) strain ε_{xx}.

exposure time, it is advised to change by small amounts. Larger changes result in higher uncertainty (as presented in figure 7). Moreover, it is interestingly noted from figure 8 that even at the same Δ, higher slopes (i.e. higher sensitivity of error) take place at higher reference exposure times (when comparing 20 000 μs to 45 000 μs and 50 000 μs). This can be explained using table 2, which shows that the images with exposure times of 45 000 μs and 50 000 μs have $Z_2 = 255$. Such images have more than 5% of their pixels already saturated and thus are more likely to add more errors into DIC when exposure time is changed.

When it comes to high temperature, it is once more observed that when $\Delta < 50$ exposure time cannot be changed at a fixed temperature, and in all cases when exposure time can be changed $\Delta > 50$. Also, it is noted that since images get brighter at high temperature due to thermal radiation, it is advised to set the initial exposure time low

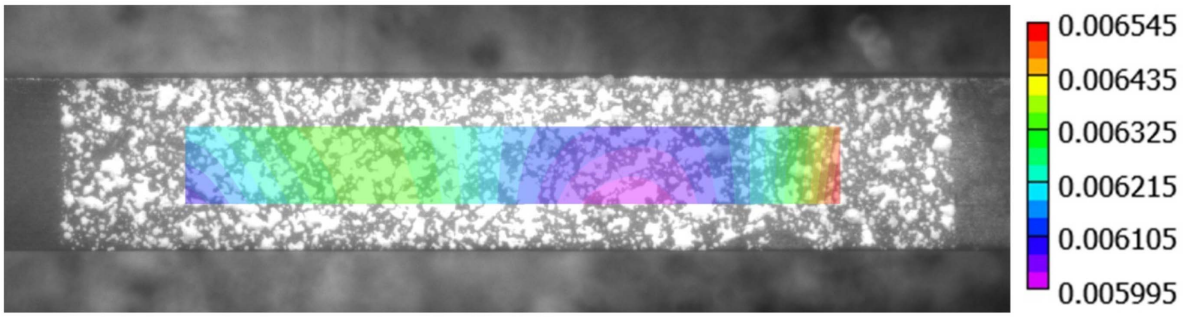

Figure 14. Non-uniform thermal strain from correlation of 45 000 μs at room temperature against 30 000 μs at 1600 °C.

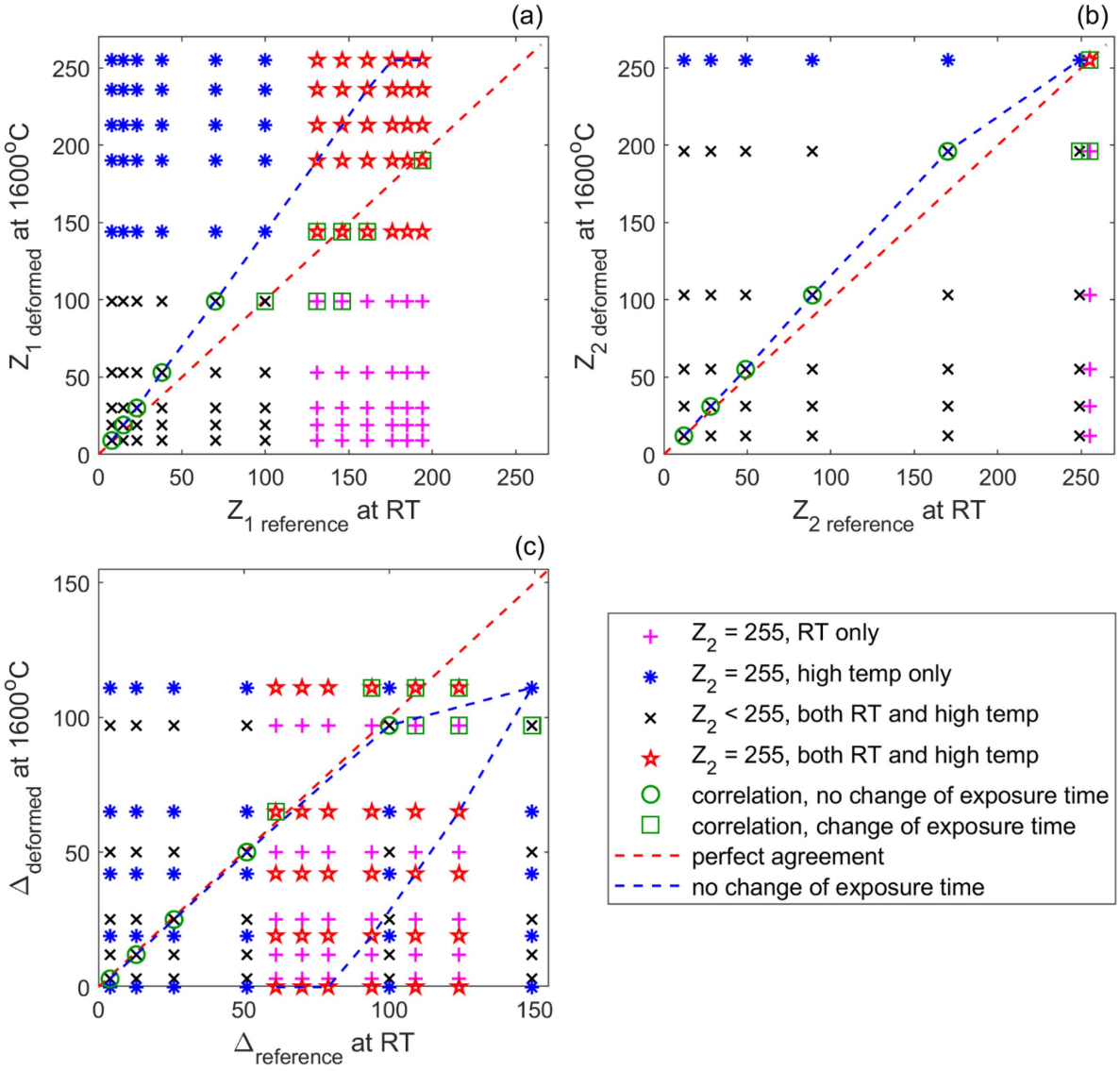

Figure 15. Correlation of image pairs at RT vs 1600 °C when investigating via (a) Z_1, (b) Z_2 and (c) Δ.

at room temperature in order to avoid saturation at high temperature.

In the event when images glow brightly at high temperatures, camera settings which produced sufficient contrast at low temperature may produce saturated images at high temperatures. For those situations, in order to salvage some data, it may be better to reduce the exposure time rather than lose all data due to saturation. To illustrate, figure 12

shows all pairs in which an image at room temperature (horizontal axis) successfully correlated against an image at high temperature (vertical axis). The blue dashed line indicates no change of exposure time. It can be seen that for low exposure times (green circle data points), it is not necessary to change exposure time at high temperatures. However, for high initial exposure times (green square data points), the only successful correlations involved reducing exposure time at high temperature. Thus, by reducing exposure time at high temperature, a DIC user can salvage some data rather than no data, but should expect higher uncertainty as a trade-off.

Figure 15 shows Z_1, Z_2, and Δ for all 144 image pairs between room temperature and high temperature. The data are sorted into four quadrants depending on whether $Z_2 = 255$ in the room-temperature image, high-temperature image, neither, or both. Additionally, the image pairs which correlated in figure 12 are plotted as circles or squares. Each plot also includes a red dashed line, indicating no change of Z_1, Z_2, or Δ; and a blue dashed line, indicating no change of exposure time. The dashed lines include image pairs which did not successfully correlate.

Figure 15(a) shows that when neither image saturates ($Z_2 = 255$), no change of exposure time is needed; but if one or both images saturate, successful correlations occurred when the exposure time was reduced to maintain similar values of Z_1 in both images. Figure 15(b) contains many overlapping points in which one or both images have $Z_2 = 255$, but in general the successful correlations also occur when Z_2 of both images remain similar. Figure 15(c) is much messier than parts (a) or (b), but generally agrees with figure 15(a) that when neither image saturates no change of exposure time is needed, but when one or both images saturate Δ can only change and still result in successful correlation if it started relatively large (on the order of 100). Figure 15(c) also shows that changes of exposure time must be relatively small to maintain correlation.

It is known that there are other ways to manipulate brightness besides exposure time and the findings from this paper can potentially apply to most of them. In this paper, exposure time was manipulated since the tests were quasi-static. In other cases like a dynamic test, exposure time must be kept short to prevent motion blur. In that case, by using the metric of Δ, similar results are expected by (i) increasing or decreasing the amount of externally supplied light, (ii) broadening or narrowing the aperture on the lens, or (iii) increasing or decreasing the gain on the camera sensor—though it should be noted that the Vic-3D documentation strongly advises against using gain as a source of brightness [23].

5. Conclusions

This paper investigated the effect of changing exposure time during the use of digital image correlation (DIC) in (i) isothermal testing at room temperature, (ii) isothermal testing at high temperature, and (iii) variable temperature testing from room temperature to 1600 °C. In summary, the contrast of an image can be quickly judged by the metric of delta (Δ), which takes the difference between a typical dark pixel (Z_1) and a typical bright pixel (Z_2), spanning 90% of all pixels in the image. As long as $\Delta > 50$ and Z_2 does not equal 255 (for an 8-bit camera), exposure time can be changed in the middle of test, although it results in higher uncertainty. In order to minimize uncertainty and maximize the ability to correlate with different exposure times, Δ should be as high as possible in the room-temperature image. Although changes to exposure time should be minimal in order to minimize uncertainty, in some cases it may be better to change exposure time in order to salvage some data rather than lose the data completely.

Acknowledgments

This work was funded in part by a grant from NASA's Marshall Space Flight Center (award #80MSFC18M0009) and by the Utah State University Office of Research and Graduate Studies.

ORCID iD

Ryan B Berke https://orcid.org/0000-0003-0612-8665

References

[1] Sutton M A, Orteu J J and Schreier H 2009 *Image Correlation for Shape, Motion and Deformation Measurements: Basic Concepts,Theory and Applications* (New York: Springer) (https://doi.org/10.1007/978-0-387-78747-3)

[2] Pan B 2018 Digital image correlation for surface deformation measurement: historical developments, recent advances and future goals *Meas. Sci. Technol.* **29** 082001

[3] Pan B, Qian K, Xie H and Asundi A 2009 Two-dimensional digital image correlation for in-plane displacement and strain measurement: a review *Meas. Sci. Technol.* **20** 062001

[4] Gradl P R 2016 Digital image correlation techniques applied to large scale rocket engine testing *52nd AIAA/SAE/ASEE Joint Propulsion Conf.* (https://doi.org/10.2514/6.2016-4977)

[5] Wang X, Pan Z, Fan F, Wang J, Liu Y, Mao S X, Zhu T and Xia S 2015 Nanoscale deformation analysis with high-resolution transmission electron microscopy and digital image correlation *J. Appl. Mech.* **82** 121001–9

[6] Sabaté N, Vogel D, Gollhardt A, Marcos J, Gràcia I, Cané C and Michel B 2006 Digital image correlation of nanoscale deformation fields for local stress measurement in thin films *Nanotechnology* **17** 5264

[7] Li L-G, Liang J, Guo X, Guo C, Hu H and Tang Z-Z 2014 Full-field wing deformation measurement scheme for in-flight cantilever monoplane based on 3D digital image correlation *Meas. Sci. Technol.* **25** 065202

[8] Rizo-Patron S and Sirohi J 2017 Operational modal analysis of a helicopter rotor blade using digital image correlation *Exp. Mech.* **57** 367–75

[9] Yoneyama S 2016 Basic principle of digital image correlation for in-plane displacement and strain measurement *Adv. Compos. Mater.* **25** 105–23

[10] Thai T Q 2018 Importance of exposure time on digital image correlation (DIC) at extreme temperatures *PhD Thesis* Utah State University

[11] Reu P 2013 Calibration: a good calibration image *Exp. Tech.* **37** 1–3

[12] Grant B M B, Stone H J, Withers P J and Preuss M 2009 High-temperature strain field measurement using digital image correlation *J. Strain Anal. Eng. Des.* **44** 263–71
[13] Chen X, Xu N, Yang L and Xiang D 2012 High temperature displacement and strain measurement using a monochromatic light illuminated stereo digital image correlation system *Meas. Sci. Technol.* **23** 125603
[14] Novak M D and Zok F W 2011 High-temperature materials testing with full-field strain measurement: experimental design and practice *Rev. Sci. Instrum.* **82** 115101
[15] Pan B, Wu D, Wang Z and Xia Y 2011 High-temperature digital image correlation method for full-field deformation measurement at 1200 °C *Meas. Sci. Technol.* **22** 015701
[16] Blaber J, Adair B S and Antoniou A 2015 A methodology for high resolution digital image correlation in high temperature experiments *Rev. Sci. Instrum.* **86** 035111
[17] Wang W, Xu C, Jin H, Meng S, Zhang Y and Xie W 2017 Measurement of high temperature full-field strain up to 2000 °C using digital image correlation *Meas. Sci. Technol.* **28** 035007
[18] Berke R B and Lambros J 2014 Ultraviolet digital image correlation (UV-DIC) for high temperature applications *Rev. Sci. Instrum.* **85** 045121
[19] Thai T Q, Hansen R S, Smith A J, Lambros J and Berke R B 2019 Importance of exposure time on DIC measurement uncertainty at extreme temperatures *Exp. Tech.* **43** 261–71
[20] OMEGA Engineering, Inc 2020 Thermocouple type k reference table *Thermocouple Types* (https://www.omega.com/en-us/resources/thermocouple-types)
[21] Reu P 2015 All about speckles: contrast *Exp. Tech.* **39** 1–2
[22] Reu P 2013 Stereo-rig design: lighting—part 5 *Exp. Tech.* **37** 1–2
[23] Simonsen M Vic-3d application note: using gain in vic-snap